Electronic Supplementary Material (ESI) for Journal of Materials Chemistry C.

Protein-based (bio)materials: a way toward high-performance graphene enzymatic biosensors.

Alessandro Silvestri[1], Faxing Wang[2], Xinliang Feng[2], Aitziber L. Cortajarena[1,3]*, Maurizio Prato[1,3,4]**

1. Center for Cooperative Research in Biomaterials (CIC BiomaGUNE), Basque Research and Technology Alliance (BRTA), Donostia-San Sebastián, 20014, Spain

2. Faculty of Chemistry and Food Chemistry and Center for Advancing Electronics Dresden (cfaed), Technische Universität Dresden, Dresden, 01062, Germany

3. Ikerbasque, Basque Foundation for Science, Bilbao, 48009, Spain

4. Department of Chemical and Pharmaceutical Sciences, Universitá degli Studi di Trieste, Trieste, 34127, Italy).

Supporting Information

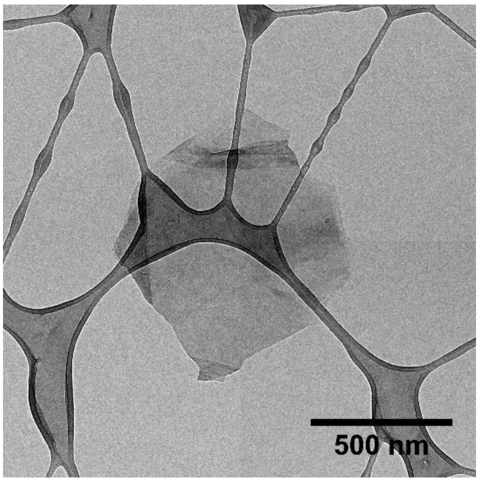

Figure S1. TEM micrograph of the electrochemically exfoliated graphene (EEG).

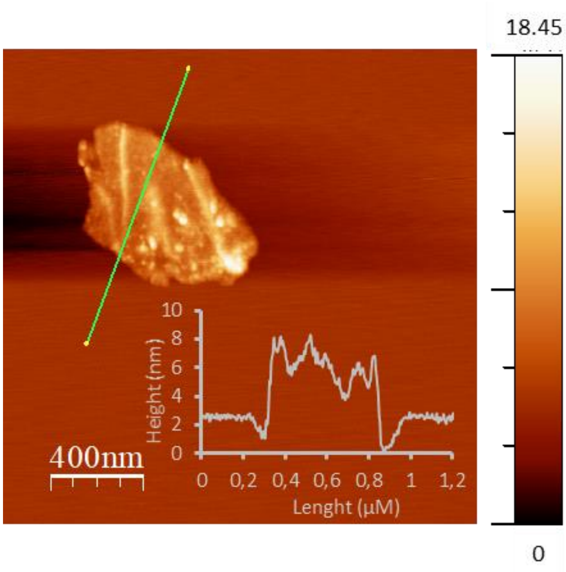

Figure S2. AFM height micrograph of the electrochemically exfoliated graphene (EEG). Inset: height profile of EEG flake.

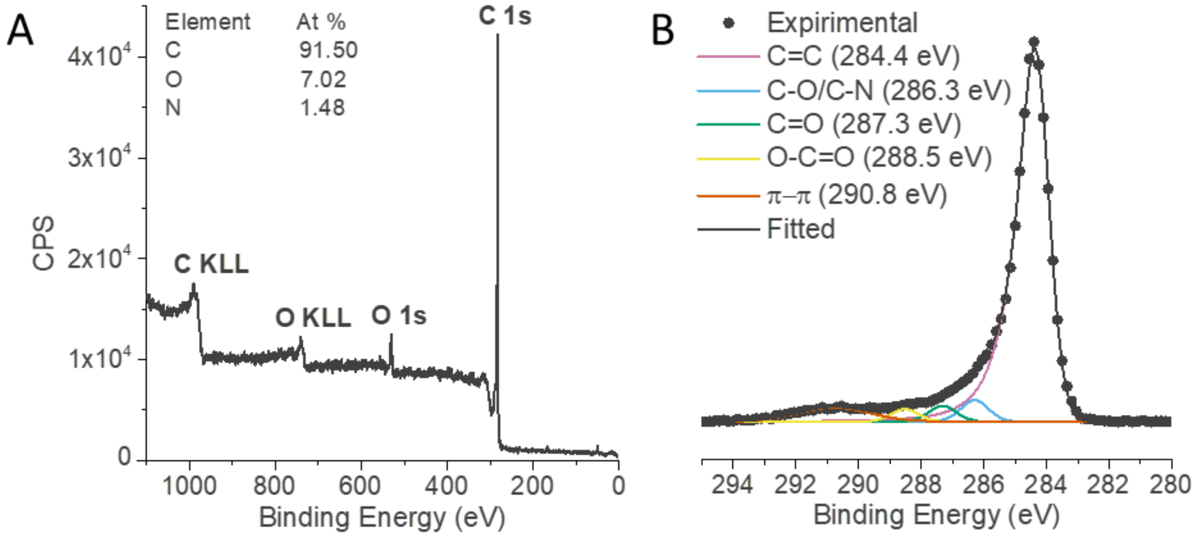

Figure S3. XPS characterization of the pristine EEG: a) Survey spectrum and elemental composition, b) deconvoluted high resolution C 1S core spectrum.

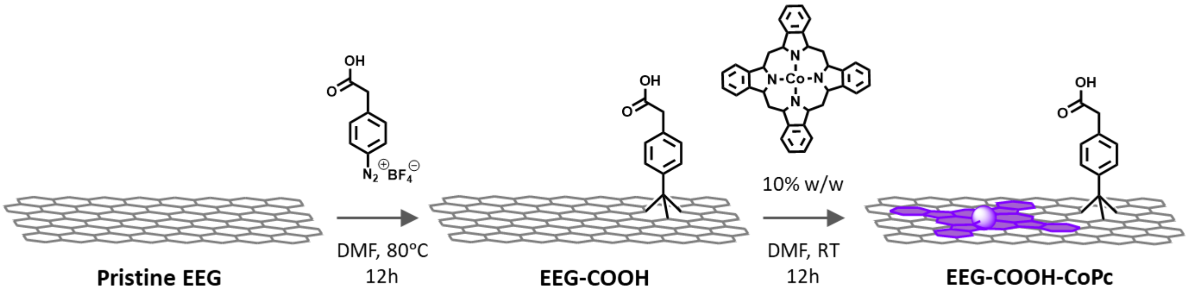

Figure S4. Schematic representation of the synthesis of the electrocatalytic graphene ink.

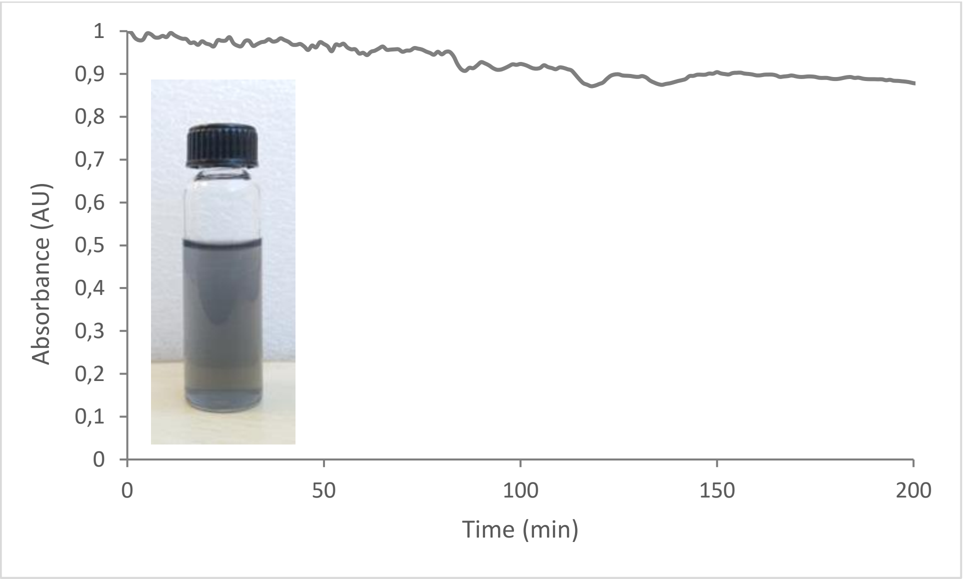

Figure S5. Sedimentation rate of the electrocatalytic graphene ink monitored by the absorption of the solution at 660 nm.

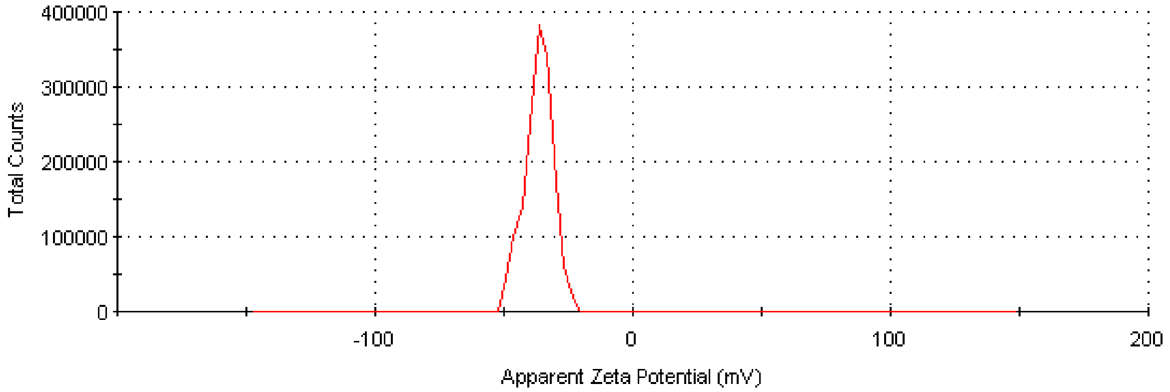

Figure S6. ζ-potential of the electrocatalytic graphene ink.

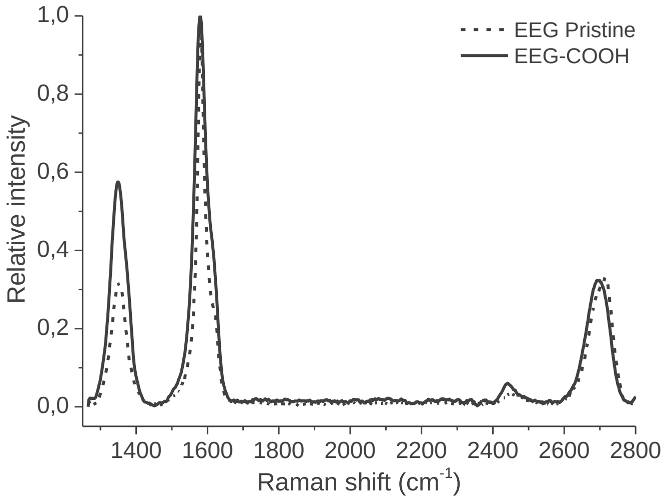

Figure S7. Raman Spectra of the graphene pristine and after the reaction with phenylacetic acid diazonium salts. The increase of the D band intensity (1350 cm^{-1}) testify the successful outcome of the reaction.

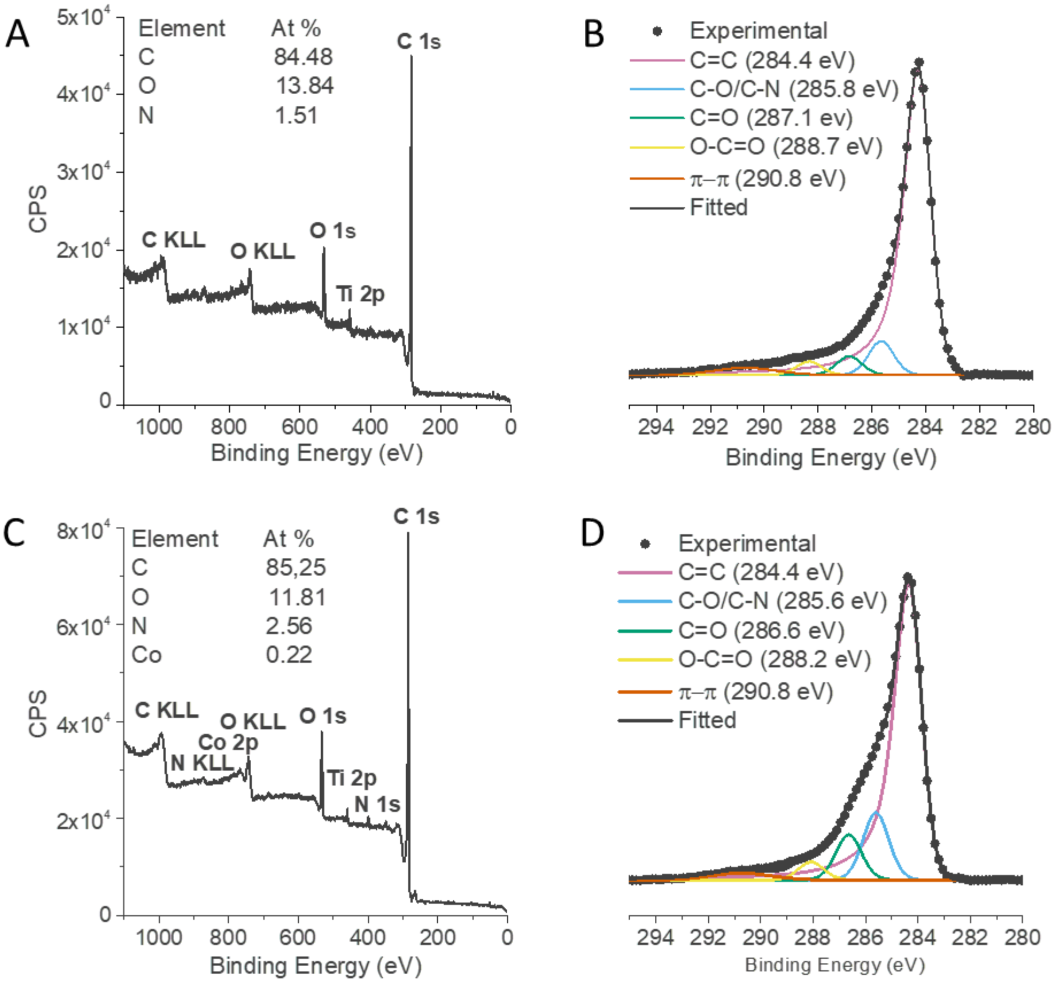

Figure S8. XPS characterization of EEG-COOH (a,b), EEG-COOH-CoPC (c,d): a-c) Survey spectra and elemental composition, b-d) deconvoluted high resolution C 1S core spectrum.

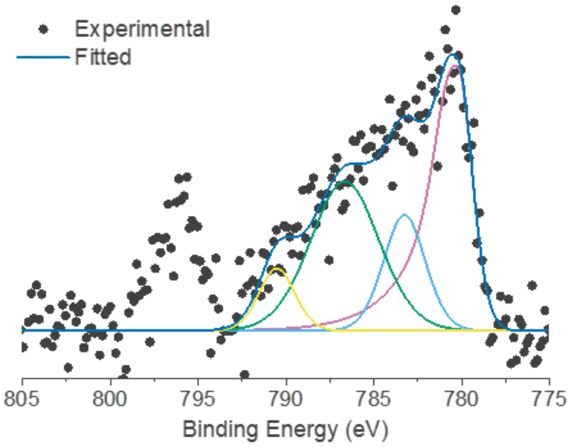

Figure S9. Deconvoluted high resolution XPS spectrum of Co 2p core of EEG-COOH-CoPC

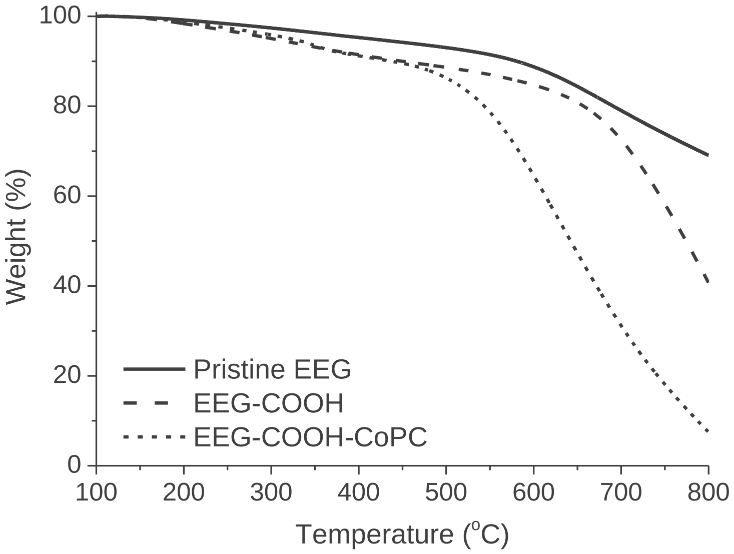

Figure S10. TGA analysis of EEG, EEG-COOH, EEG-COOH-CoPC indicating subsequent weight losses after each functionalization stage.

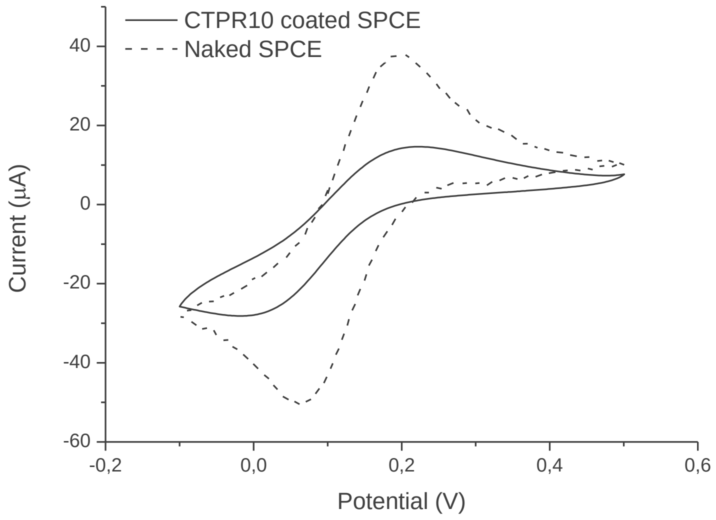

Figure S11. Cyclic voltammogram of $[Fe(CN)_6]^{3-}$ 1 mM in presence (solid line) and absence (dashed line) of CTPR10 protein film (scan rate 20 mV s^{-1}).

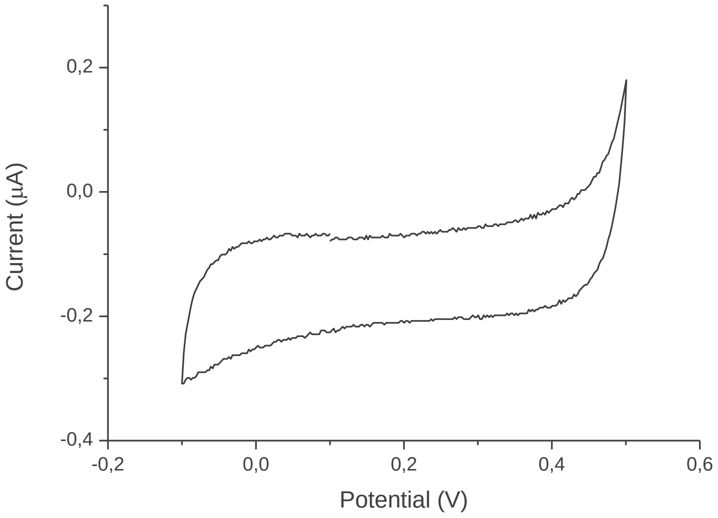

Figure S12. Cyclic voltammogram of a SPCE coated with CTPR10 protein film in PBS (scan rate 20 mV s^{-1}).

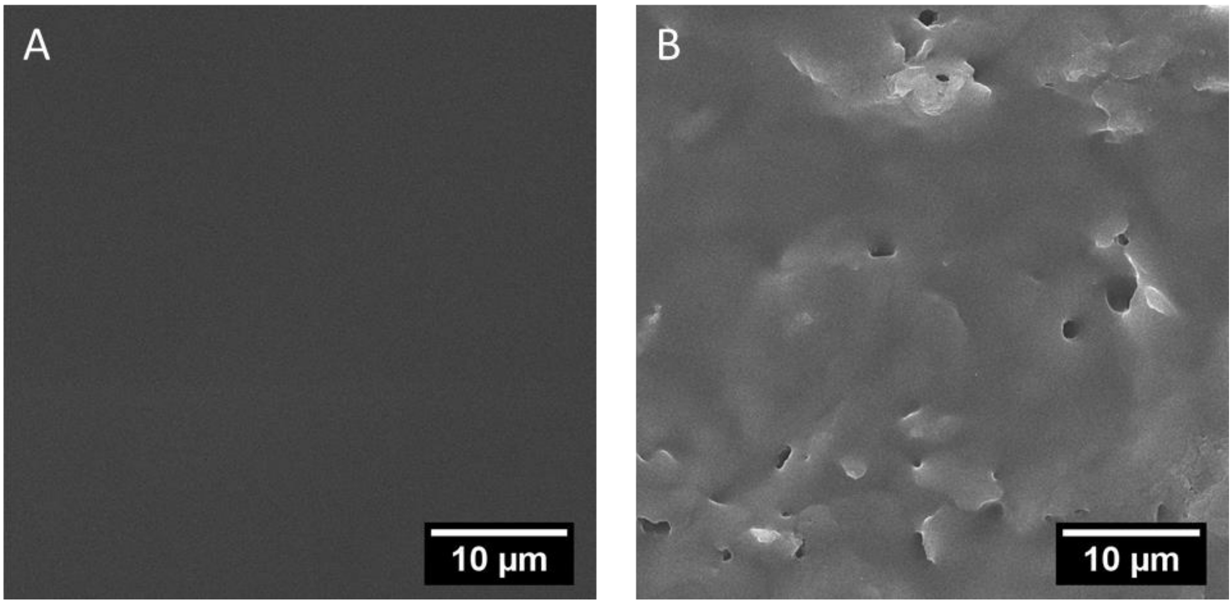

Figure S13. SEM micrographs of CTPR10-LOx thin film before (a) and after (b) amperometric measurement.

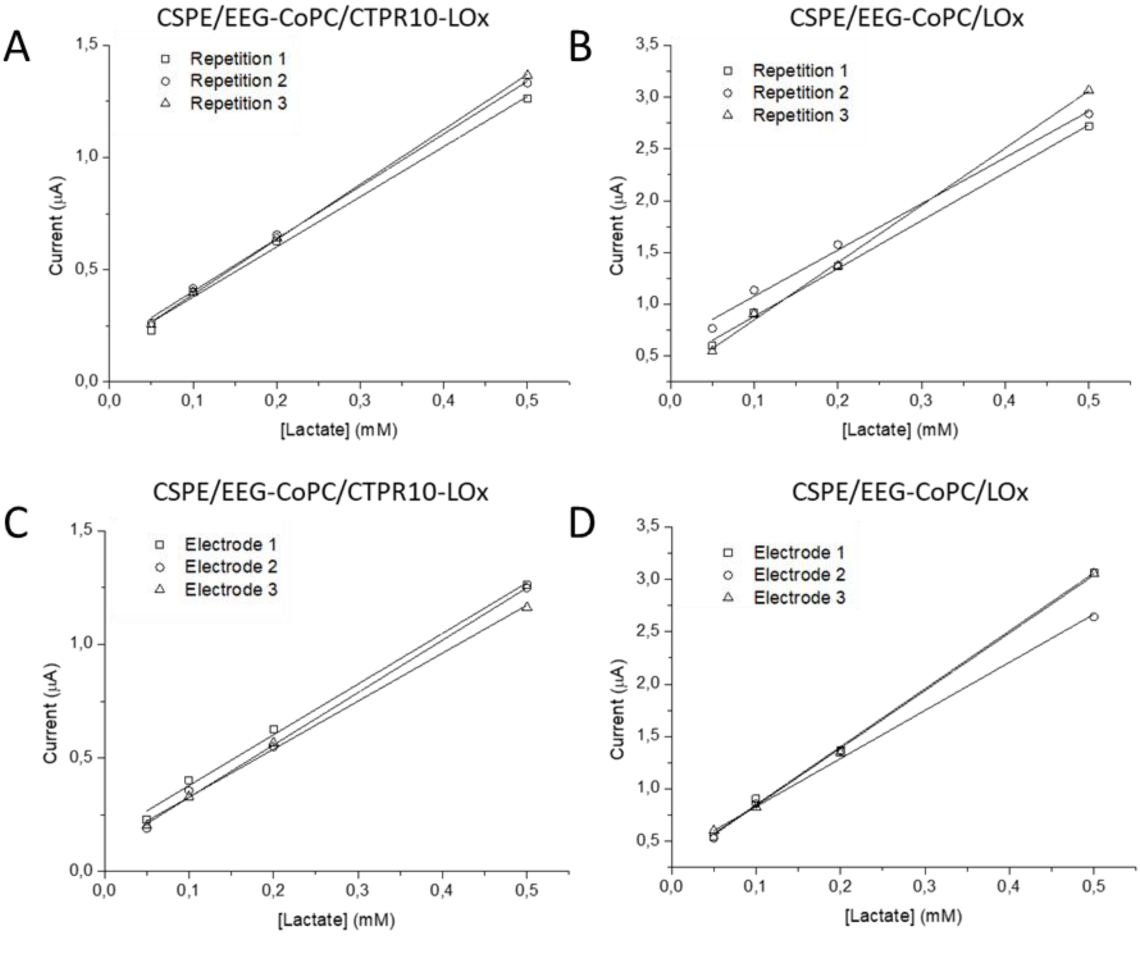

Figure S14. Repeatability (a-b) and reproducibility (c-d) of LOX-CTPR10/EEG-CoPC and LOX/EEG-CoPC (control). a-b) Calibration lines obtained from three consecutive FIAs on the same C-SPE electrode modified with the ink. c-d) Calibration lines obtained from three different electrodes.

Table S1. Comparison of the performances of the herein presented LOx-based biosensor, with the literature benchmark

Electrode design	Sensitivity (µA mM^{-1})	LOD (µM)	Linear range (µM)	Response time (s)	Shelf-life	Ref
GC/Poly-L-Lysine/LOx/Poly(4-styrenesulfonate)	-	0.1	300-1k	5	40 % after 60 days (4°C)	1
Pt printed electrod/LOx	-	8	8-1k	60	30 % after 4 days (4°C)	2
Pt/Phenyl-ethilendiamine/LOx/PVC	0.009	-	1k-150k	60	100 % after 280 days (4 °C)	3
GC/Osmium-polymer/LOx	1.02	50	1k-9k	10	7 days	4
ITO/Polyaniline-co-fluoroaniline film/LOx	1.18	100	1k-5.5k	50	50% after 26 days (4 °C)	5
Dimethylferrocene-poly(ethylenimine) hydrogel/LOx	45	3	0-5k	-	100% after 21 days (4 °C)	6
Polyphenyldiamine/LOx	-	2	0-2k	4	5 days	7
Protein stabilized						
Pt/Polypirrole/BSA/LOx	0.007	15	0-20k	-	60% after 120 days at (4 °C) 86% after 2 days (28 °C)	8
Pt/albumin-mucin hydrogel/LOx/Polycarbonate	0.537	0.8	2-1k	50	70 % after 360 days (4 °C)	9
Pt/Lox/Gelatine	5	5	0-30k	20-30	85 % after 300 days (RT)	10
CNM based						
N-CNT/LOx/Nafion	40 µA cm^{-2} mM^{-1}	4.1	14-325	2	20% after 90 days (4 °C)	11
Gpaper/MoS$_2$/Cu/LOx	83 µA cm^{-2} mM^{-1}	0.1	10-18.4k	3	80% after 30 days (4 °C)	12
SPE/rGO-3,4DHS/LOx	0.6 µA cm^{-2} mM^{-1}	2.9	10-800	-	85% after 30 days (4 °C)	13
SPE/rGO/K$_3$[FeCN)$_6$]/LOx	42 µA cm^{-2} mM^{-1}	60	500-15k	10	82% after 15 days (4 °C)	14
Pt/rGO/CNT/AuNPs/LOx	35 µA cm^{-2} mM^{-1}	2.3	50-100k	100	100 % after 30 days (4 °C)	15
Carboxymethyl cellulose/K$_3$[FeCN)$_6$]/LOx	-	1000	1k-50k	50	7 days (RT)	16
Silica sol-gel/ MWCNTs	6.31	0.3	200-2k	5	90% after 30 days (RT)	17
Au/MWCNT/Chitosane/LOx-HPR/Chitosane	0.00347	1.66	5-350	65	90 % after 450 days (RT)	18
SPE/EEG-CoPC/Lox	41.46 µA cm^{-2} mM^{-1}	0.25	0.25-1k	8	10% after 10 days (RT)	This work
SPE/EEG-CoPC/CTPR10-LOx	17.66 µA cm^{-2} mM^{-1}	1.24	1-1k	8	70 % after 200 days (RT)	This work

References

(1) Mizutani, F.; Yabuki, S.; Hirata, Y. Amperometric L-Lactate-Sensing Electrode Based on a Polyion Complex Layer Containing Lactate Oxidase. Application to Serum and Milk Samples. *Analytica Chimica Acta* **1995**, *314* (3), 233–239. https://doi.org/https://doi.org/10.1016/0003-2670(95)00278-8.

(2) Goriushkina, T. B.; Soldatkin, A. P.; Dzyadevych, S. v. Application of Amperometric Biosensors for Analysis of Ethanol, Glucose, and Lactate in Wine. *Journal of Agricultural and Food Chemistry* **2009**, *57* (15), 6528–6535. https://doi.org/10.1021/jf9009087.

(3) Yang, Q.; Atanasov, P.; Wilkins, E. Needle-Type Lactate Biosensor1This Paper Was Presented at the Fifth World Congress on Biosensors, Berlin, Germany, 3–5 June 1998.1. *Biosensors and Bioelectronics* **1999**, *14* (2), 203–210. https://doi.org/https://doi.org/10.1016/S0956-5663(98)00109-2.

(4) Park, T.-M.; Iwuoha, E. I.; Smyth, M. R.; Freaney, R.; McShane, A. J. Sol-Gel Based Amperometric Biosensor Incorporating an Osmium Redox Polymer as Mediator for Detection of l-Lactate. *Talanta* **1997**, *44* (6), 973–978. https://doi.org/https://doi.org/10.1016/S0039-9140(96)02164-9.

(5) Suman, S.; Singhal, R.; Sharma, A. L.; Malthotra, B. D.; Pundir, C. S. Development of a Lactate Biosensor Based on Conducting Copolymer Bound Lactate Oxidase. *Sensors and Actuators B: Chemical* **2005**, *107* (2), 768–772. https://doi.org/https://doi.org/10.1016/j.snb.2004.12.016.

(6) Hickey, D. P.; Reid, R. C.; Milton, R. D.; Minteer, S. D. A Self-Powered Amperometric Lactate Biosensor Based on Lactate Oxidase Immobilized in Dimethylferrocene-Modified LPEI. *Biosensors and Bioelectronics* **2016**, *77*, 26–31. https://doi.org/https://doi.org/10.1016/j.bios.2015.09.013.

(7) Palmisano, F.; Centonze, D.; Zambonin, P. G. An in Situ Electrosynthesized Amperometric Biosensor Based on Lactate Oxidase Immobilized in a Poly-o-Phenylenediamine Film: Determination of Lactate in Serum by Flow Injection Analysis. *Biosensors and Bioelectronics* **1994**, *9* (7), 471–479. https://doi.org/https://doi.org/10.1016/0956-5663(94)90009-4.

(8) Palmisano, F.; Rizzi, R.; Centonze, D.; Zambonin, P. G. Simultaneous Monitoring of Glucose and Lactate by an Interference and Cross-Talk Free Dual Electrode Amperometric Biosensor Based on Electropolymerized Thin Films. *Biosensors and Bioelectronics* **2000**, *15* (9), 531–539. https://doi.org/https://doi.org/10.1016/S0956-5663(00)00107-X.

(9) Romero, M. R.; Ahumada, F.; Garay, F.; Baruzzi, A. M. Amperometric Biosensor for Direct Blood Lactate Detection. *Analytical Chemistry* **2010**, *82* (13), 5568–5572. https://doi.org/10.1021/ac1004426.

(10) Khan, G. F.; Wernet, W. Design of Enzyme Electrodes for Extended Use and Storage Life. *Analytical Chemistry* **1997**, *69* (14), 2682–2687. https://doi.org/10.1021/ac961208z.

(11) Goran, J. M.; Lyon, J. L.; Stevenson, K. J. Amperometric Detection of L-Lactate Using Nitrogen-Doped Carbon Nanotubes Modified with Lactate Oxidase. *Analytical Chemistry* **2011**, *83* (21), 8123–8129. https://doi.org/10.1021/ac2016272.

(12) Wang, Z.; Dong, S.; Gui, M.; Asif, M.; Wang, W.; Wang, F.; Liu, H. Graphene Paper Supported MoS2 Nanocrystals Monolayer with Cu Submicron-Buds: High-Performance Flexible Platform for Sensing in Sweat. *Analytical Biochemistry* **2018**, *543*, 82–89. https://doi.org/https://doi.org/10.1016/j.ab.2017.12.010.

(13) Bravo, I.; Revenga-Parra, M.; Weber, K.; Popp, J.; Pariente, F.; Lorenzo, E. One-Step Reduced/Quinone Functionalized Graphene Oxide as Reagentless Lactate Biosensing Platform. *Sensors and Actuators B: Chemical* **2018**, *267*, 533–541. https://doi.org/https://doi.org/10.1016/j.snb.2018.03.170.

(14) Tu, D.; He, Y.; Rong, Y.; Wang, Y.; Li, G. Disposable L-Lactate Biosensor Based on a Screen-Printed Carbon Electrode Enhanced by Graphene. *Measurement Science and Technology* **2016**, *27* (4), 045108. https://doi.org/10.1088/0957-0233/27/4/045108.

(15) Hashemzadeh, S.; Omidi, Y.; Rafii-Tabar, H. Amperometric Lactate Nanobiosensor Based on Reduced Graphene Oxide, Carbon Nanotube and Gold Nanoparticle Nanocomposite. *Microchimica Acta* **2019**, *186* (10), 680. https://doi.org/10.1007/s00604-019-3791-0.

(16) Sato, N.; Okuma, H. Amperometric Simultaneous Sensing System for d -Glucose and l -Lactate Based on Enzyme-Modified Bilayer Electrodes. **2006**, *565*, 250–254. https://doi.org/10.1016/j.aca.2006.02.041.

(17) Song, Z.; Zhao, Z.; Qin, X.; Huang, J.; Shi, H.; Wu, B.; Chen, Q. Highly Sensitive Choline Biosensor Based on Carbon Nanotube-Modified Pt Electrode Combined with Sol-Gel Immobilization. *Frontiers of Chemistry in China* **2007**, *2* (2), 146–150. https://doi.org/10.1007/s11458-007-0030-8.

(18) Monošík, R.; Streďanský, M.; Greif, G.; Šturdík, E. A Rapid Method for Determination of L-Lactic Acid in Real Samples by Amperometric Biosensor Utilizing Nanocomposite. *Food Control* **2012**, *23* (1), 238–244. https://doi.org/https://doi.org/10.1016/j.foodcont.2011.07.021.